

Characterization of Microstructure and Mechanical Behaviour in Activated Tungsten Inert Gas Welded Dissimilar AA Joint of AA 5083 and AA 6061 Alloys

Sundar VettumPerumal¹ · VijayAnanth Suyamburajan¹ · Vettivel Singaravel Chidambaranathan² · Leema Nelson³

Received: 17 August 2023 / Accepted: 21 September 2023
© The Institution of Engineers (India) 2023

Abstract Aluminium alloys have a wide range of use in the manufacturing industries. Fusion welding procedures frequently use metal inert gas and tungsten inert gas (TIG) welding to combine aluminium alloys (AA). Overdue to AA's high expansion coefficient, high thermal conductivity and high electrical conductivity, it is more challenging to weld AA than steel. The capacity of TIG welding thick structures cannot be welded in one pass. Activated TIG (A-TIG), a novel development in TIG welding, has been created. With this technique, a single pass results in an ultra-deep penetration. The A-TIG welding procedure for combining AA 6061 and AA 5083 is described in this publication. The varied welding parameters' effects such as welding current, flux and filler rod for improving hardness have also been explored. Compared to conventional TIG welding, the TiO₂ flux used in A-TIG welding enhanced the depth of penetration DOP and lowered the bead width. The TiO₂ flux significantly improved weld hardness and reduced bead width. EDS and SEM analysis revealed changes in alloy composition and microstructure. This study successfully

established dissimilar joints between AA 6061 and 5083 using A-TIG welding, with enhanced DOP and mechanical properties. The TiO₂ flux played a vital role in altering surface tension and improving weld characteristics. The findings contribute to the understanding of A-TIG welding in dissimilar alloys, specifically AA 6061 and 5083.

Keywords Aluminium alloys · TIG and A-TIG welding · Welding parameters · TiO₂ flux · Mechanical properties · Microstructure

Introduction

Due to their widespread use in all industrial applications, aluminium alloys (AA) were chosen as a viable material for TIG welding. The special qualities of AA include being the most versatile, affordable, and visually appealing material with extensive engineering applications [1]. The welding process parameters, as well as the material's chemical composition and manufacturing process, all have a major impact on the strength of weld joints. Generally speaking, AA is divided into the effects of the 1XXX through 9XXX series according to the alloying element's composition. In the process of A-TIG welding, a flux layer is created from a mix of volatile and inorganic elements. The performance of traditional TIG welding is improved by A-TIG welding [2]. Enhancing weld penetration by applying a fine layer of flux on the surface is referred to as active flux TIG (ATIG). This innovative welding technique was initially pioneered in the 1960s at the PATON Welding Institute in Ukraine. Subsequent research efforts in various research centres further contributed to the development and adoption of this method in industrial applications [3]. Before welding, a thin layer of flux is applied evenly across the joint. This flux primarily consists of finely

✉ VijayAnanth Suyamburajan
ssvijayananth@gmail.com

Vettivel Singaravel Chidambaranathan
scvettivel@ccet.ac.in

Leema Nelson
leema.nelson@chitkara.edu.in

¹ Department of Mechanical Engineering, VELS Institute of Science Technology and Advanced Studies, Chennai, Tamilnadu, India

² Department of Mechanical Engineering, Chandigarh College of Engineering and Technology, Degree Wing, Sector 26, Chandigarh 160019, India

³ Chitkara University Institute of Engineering and Technology, Chitkara University, Rajpura, Punjab, India

powdered oxides and halides. Initially, the powdered flux is transformed into a slurry by adding a suitable organic solvent, with common choices being carbinol, ethanol, or acetone. The solvent is carefully mixed with the activated flux in the correct proportions, ensuring that it evaporates during the process, leaving behind a protective flux layer on the joint's surface. The A-TIG welding method eliminates the need for filler wire, reduces the time required for groove preparation, and significantly enhances weld penetration [4]. Pulsed TIG welding is a widely employed welding method known for its numerous advantages when compared to the conventional TIG welding process. These advantages encompass precise control of heat input, minimized distortion, a smaller heat affected zone (HAZ), decreased residual stresses, and reduced micro-segregation [5]. TIG spot welding is a specialized TIG welding technique primarily used for spot welding thin sheets or foils. It creates small, localized welds without significant heat input, making it suitable for delicate or heat-sensitive materials [6]. Important considerations for improving weld strength are welding parameters [7]. Applications of ATIG welding include the fabrication of pressure vessels and tube-to-tube sheets in heat exchangers, power and chemical industries, hydraulic cylinders and undercarriage legs in the aerospace industry, and pipes and tubes in the nuclear industry [8]. The use of this technology is restricted in some circumstances due to factors including its use, particularly in industries, and poor metallurgical and mechanical qualities. When using different kinds of steel and supplied fluxes for A-TIG welding, varied outcomes are obtained. It is a procedure that involves applying a thin layer of flux over the joint region prior to welding, and it increases weld penetration while maintaining the same parameters as traditional TIG welding [9]. A-TIG welding process variables include welding current, filler material, travel speed, shielding gas flow rate, and electrode diameter, which impact the weldment's microstructure and strength. Three variables-welding current, flux, and filler material-have been chosen for the experiment. The literature has reported that these parameters play a vital role in obtaining better mechanical properties [6].

AA 6061 is used in pipe railing, furniture, automotive parts, hospital medical equipment, highway signs, kitchen equipment, machine parts, and marine applications [7]. AA5083 is a non-heat-treatable magnesium alloy with excellent corrosion resistance and moderate strength. Welding AA 5083 can be a bit challenging due to its sensitivity to heat and potential for cracking, especially in thick sections. However, with proper welding techniques

and filler materials, successful welds can be achieved. It is often used in marine industry, transportation, pressure vessels and cryogenic applications [10]. AA 5083 used in marine industry, transportation. TiO_2 , SiO_2 , Al_2O_3 , CaO and Cr_2O_3 have all been utilized as oxidizing fluxes in the A-TIG welding technique to join stainless steel 304 plates. Cr_2O_3 , TiO_2 , and SiO_2 were found to have a substantial impact on the in-depth penetration [11]. Flux's main function is to confine the arc plasma and change the surface tension gradient's direction to point toward the weld location, enhancing the weld's penetration [9]. Compared to other factors, the welding current has a more significant impact on the weld deposition area [12]. A lot of research has been done on welding steel and aluminium together [13]. However, research has shown that not much work has been done on AA A-TIG welding. On AA 5083/AA 6061, however, no documented work has been made. The purpose of this essay is to draw attention to the importance of aluminium alloys (AA) in industrial settings, specifically their suitability for TIG welding because of their adaptability, affordability, and aesthetic appeal. As AA is divided into different series depending on alloying elements, it also examines the effects of welding process factors, material composition, and manufacturing procedures on weld joint strength [14]. In order to improve the performance of conventional TIG welding, activated TIG (A-TIG) welding employs a flux layer made up of volatile and inorganic materials. The research also emphasizes the critical role that welding parameters play in enhancing weld strength, highlighting the impact of elements like welding current, flux, and filler material [15]. While research on welding steel and aluminium has been extensive, this paper underscores the limited attention given to AA A-TIG welding, particularly in the context of AA 5083 and AA 6061 alloys.

Chemical Composition of AA

The composition of the alloying components determines the chemical characteristics of AA. Adding chosen elements to pure aluminium greatly increases its properties and utility. The inclusion of specific components substantially improves the characteristics and utility of pure aluminium. Copper, silicon, zinc, manganese, and magnesium are some of the most common alloying

Table 1 Chemical composition of AA 5083 and AA 6061

ALLOY	Al	Mg	Mn	Si	Cr	Cu	Zn
5083	93.25	4.90	1.0	0.4	0.25	0.2	0.1
6061	97.9	1.0	–	0.6	0.2	0.28	–

Table 2 Composition of filler

Alloy weight%	Al	Mg	Mn	Si	Cu	Zn	Fe	Ti
AA 5356	Bal	4.5	0.10	0.25	10	0.10	0.40	0.20

Table 3 Input parameters

Input parameters	Fixed parameters
Weld Current(A)	200
Flux	TiO ₂
Filler material	AA 5356
Diameter(mm) of filler rod	3
Material of electrode	Tungsten
Diameter of electrode (mm)	3
Thickness of work material l(mm)	6
Shielding gas	Argon
Shield gas flow rate (lit/min)	10 s

components used with aluminium [16]. Table 1 displays the chemical compositions of AA 5083 and AA 6061.

Selection of Filler Material

Because these alloys are most frequently utilized in the production of AA products, AA 6061 and AA 5083 have been selected for this study. The choice of AA 5356 filler material and its chemical composition is a critical aspect of your experimental work. It plays a vital role in achieving the desired mechanical qualities of the weld, and its composition is carefully selected based on the specific requirements of the welding process and the materials being joined. Table 2 lists the filler material’s chemical composition.

Selection of Input Welding Parameters of A-TIG Welding

A-TIG welding process variables include welding current, filler material, travel speed, shielding gas flow rate, and electrode diameter, which impact the weldment’s microstructure and strength [17]. Table 3 displays the process parameters used for the current investigation and constant process parameters.

Materials and Methods

AA 5083 and AA 6061 were chosen as the test specimens, and a plate measuring 80 mm by 75 mm and 6 mm thick was sliced into strips. Surface contamination was removed by rough polishing with grit silicon carbide paper. TIG welding with TiO₂ flux assistance is utilized to achieve complete penetration. Activated-TIG is another name for

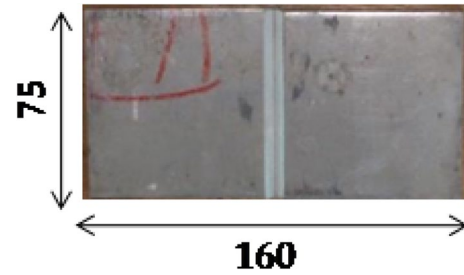


Fig. 1 Single V groove butt weld specimen preparation

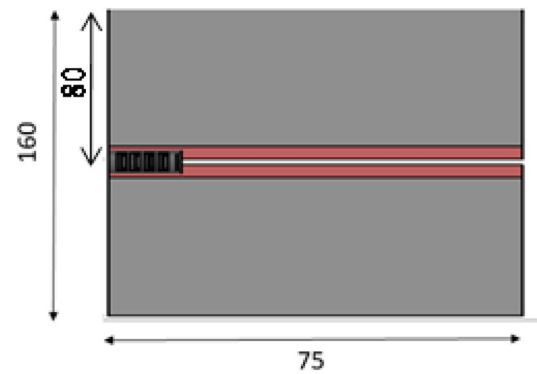


Fig. 2 Applied flux surface

it. For welding, the specimen was chamfered by a milling machine at a 60-degree angle. The single V groove butt weld specimen is shown in Fig. 1.

Preparation of Activated Flux

One of the crucial A-TIG welding procedures is preparing the activation mixture. Equations (1 and 2) are used to determine how much flux is needed for welding. Figure 2 shows the present work 160-mm-long, 12-mm-wide thick layer is deposited.

$$m = \rho * v \tag{1}$$

where

- ρ = Density of the flux,
- v = Volume of the area to be welded.

Also,

$$v = l * w * t. \tag{2}$$

where

l = Length of the weld,

w = Width of the weld and.

t = Thickness of the weld.

The samples have been welded using the above input condition of AA 6061 and AA 5083. The samples are illustrated in Fig. 3 after welding.

The result of the trial experiment showed that at the same process parameter, the penetration depth achieved by using activated flux is much higher than without flux. When using TIG welding absence of flux, the temperature coefficient of surface tension on the molten pool frequently displayed a counter value. If the surface tension at the core of the pool is lesser than the temperature at the edge of the pool, the surface tension gradient d/dT will result in centrifugal force; there will be Marangoni convection in the molten pool [18]. As a result, the molten pool surface flows effortlessly from the centre of the pool to the edge, producing a wide-ranging and narrow TIG weld. The temperature coefficient of surface tension of the molten pool was improved by TIG welding

with TiO_2 fluxes. The pool's Centre therefore had more surface tension than the pool's edge [19]. This proved that the surface tension differential drives centripetal Marangoni convection into the molten pool during this condition the fluid flow readily moves from the edge to the centre of the pool, producing a TIG weld that is both narrow and deep. Figure 4 shows the systematic diagram of marangoni force convection without and with flux.

Results and Discussion

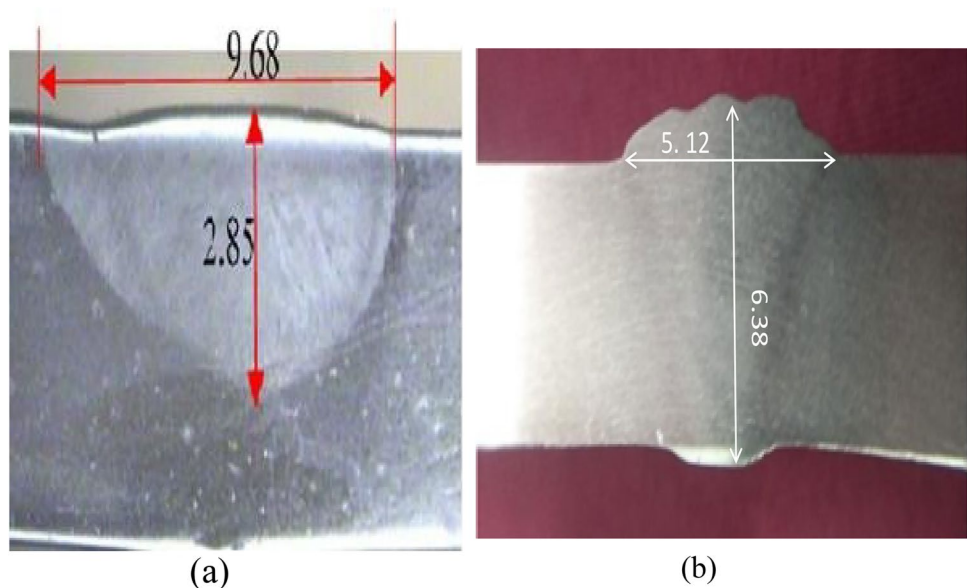
Tensile Testing

To evaluate the joint strength of the weld samples, tensile testing is done on 50 samples according to the ASTM-E8 standard. The welded samples are produced into a specimen size measuring approximately 160 mm in length and 12.5 mm in width using a wire electric discharge machine

Fig. 3 Samples after welding **a** without flux and **b** with TiO_2 flux



Fig. 4 DOP of weld **a** without flux **b** with TiO_2 flux



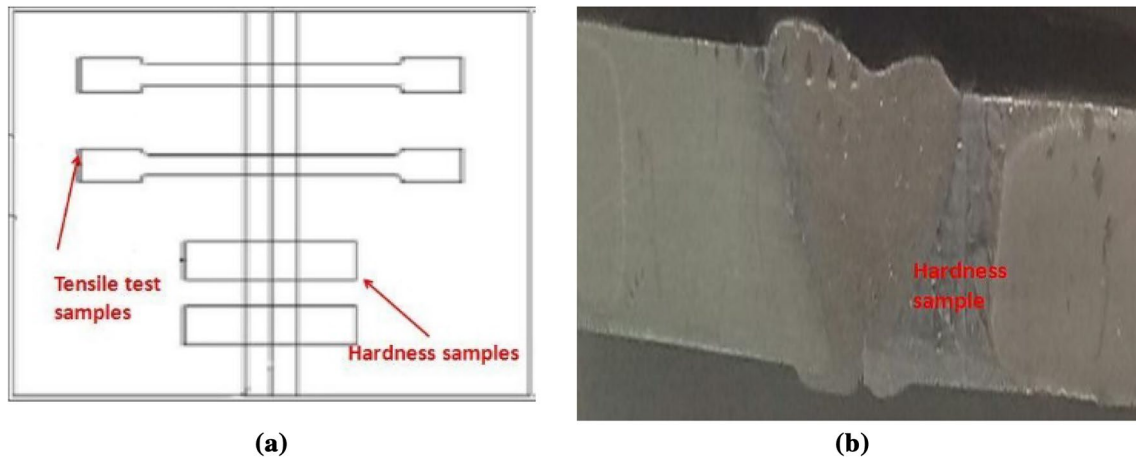


Fig. 5 a Sketch of tensile test and hardness specimen and b OM specimen

(EDM). According to the American Society for Testing and Materials, the prepared specimen is depicted in Fig. 5 (ASTM). Each specimen's data were analyzed, and the mean value was noted.

Hardness Testing

The hardness of the welded plate is measured using the Vicker hardness testing apparatus. At the interface, 50 work pieces are subjected to hardness testing. This is measured using Vickers Micro Hardness Tester at CITCO, Chandigarh, India, The test was performed according to ASTM E92. Three values were taken, and the average was recorded. Figure 6 shows the specimens for the hardness test.

Optical Microscope

The samples were mounted using a mounting press and polished using a variety of grit sizes ranging from 50 to 3000. The specimen's surface is smoothed using a diamond, alumina paste, and velvet cloth. To verify the microstructure after polishing, the samples were etched using Keller's reagent (RADICAL, model RXM 7).

Hardness

The hardness profile for A-TIG welding with flux TiO_2 and current at 200 A is shown in Fig. 5. It confirms that hardness at FZ is less than BM. Also it is confirmed that the average hardness for A-TIG with TiO_2 flux is highest compared to conventional TIG. Figure 7 shows that conventional TIG welding has the lowest hardness in FZ [10]. It could be seen that HAZ has a low hardness in each A-TIG welding with TiO_2 flux compared to FZ and BM. The low hardness in HAZ is recrystallization, due to which softening occurs as grain coarsening. The recorded hardness value at HAZ is approximately 55–60% lower as compared to BM. The HAZ of conventional TIG is softer than A-TIG welding because heat input is more as no arc constriction takes place in conventional TIG. Also, in conventional TIG at high current, the heat input per unit length is more in the area near FZ; as a result, HAZ size is more than A-TIG welding [20]. The grain gets coarsened in the β'' phase and the material get softened. Also, it is observed that in AA 6061 T6 welded joints softening of HAZ is due to different thermodynamic cycles due to heat input and heat generated during A-TIG & conventional TIG welding process.

Fig. 6 Specimen for hardness test a welded specimen and b diamond indentation

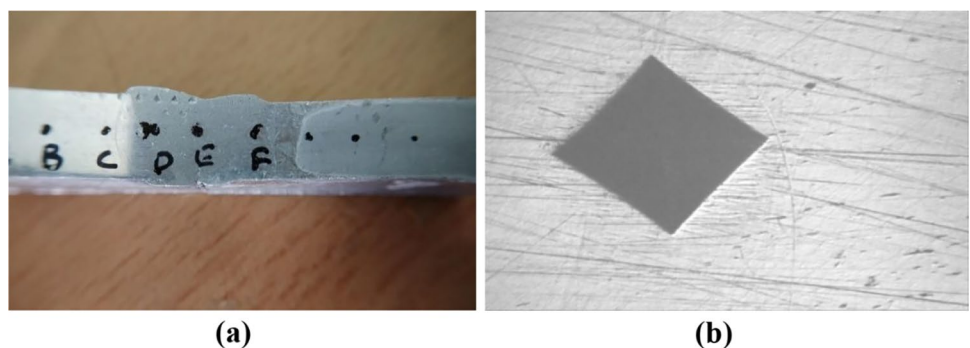
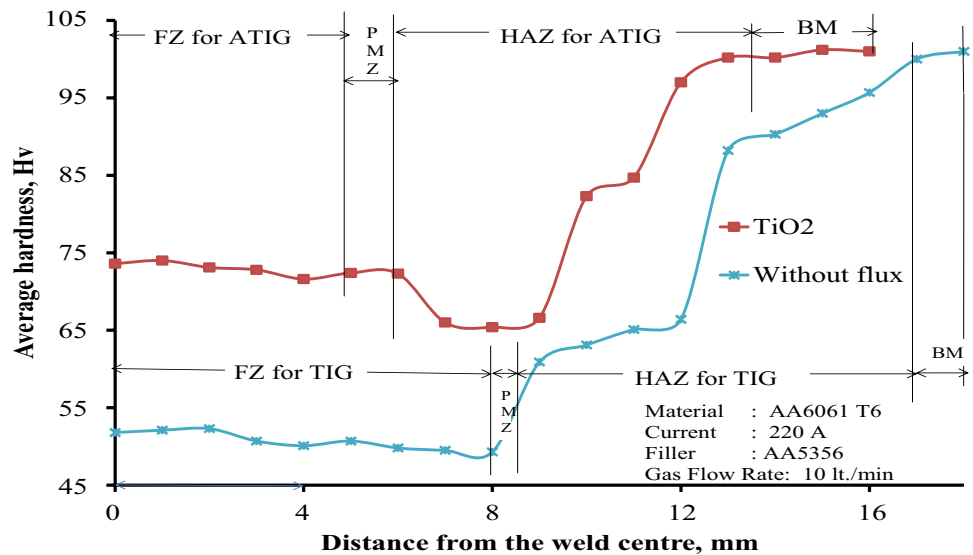


Fig. 7 Variation of hardness from the weldment to base material AA 6061 with TiO₂ flux & conventional TIG



In A-TIG welding β'' (needle shape) phase in 6061-T6 alloy changed into β' (rod shape), and further temperature increases β' changes into β phase (Mg₂Si), which resulted in softening of HAZ. In PMZ, hardness is a little more than the HAZ because of solid solution hardening and dissolution of β'' phase into β' near FZ. In A-TIG with flux, TiO₂ large amount of Ti is available at the bead and Mg is available due to filler material AA 5356; hence compound is in the weld region due to that weld region has more hardness as compared to other A-TIG welding with different fluxes.

The hardness improvement in FSW is primarily attributed to the solid-state nature of the process, which minimizes the HAZ, promotes a refined microstructure, and allows for the precipitation of strengthening phases in certain alloys. Additionally, careful optimization of process parameters is

crucial for achieving the desired hardness and mechanical properties in FSW joints [21–23]. To mitigate the negative impact of coarse grains in the FZ, it is important to carefully control welding parameters, including heat input and cooling rates, as well as select appropriate filler materials and welding techniques. Additionally, pre-weld and post-weld heat treatments may be employed to refine the grain structure and improve the overall weld quality. The specific approach to addressing coarse-grained FZs will depend on the materials being welded, the welding process used, and the intended application of the weld. AA 6061 and AA 5083 is shown in Figs. 7 and 8.

Fig. 8 Variation of hardness from the weldment to base material AA 5083 with TiO₂ flux & conventional TIG

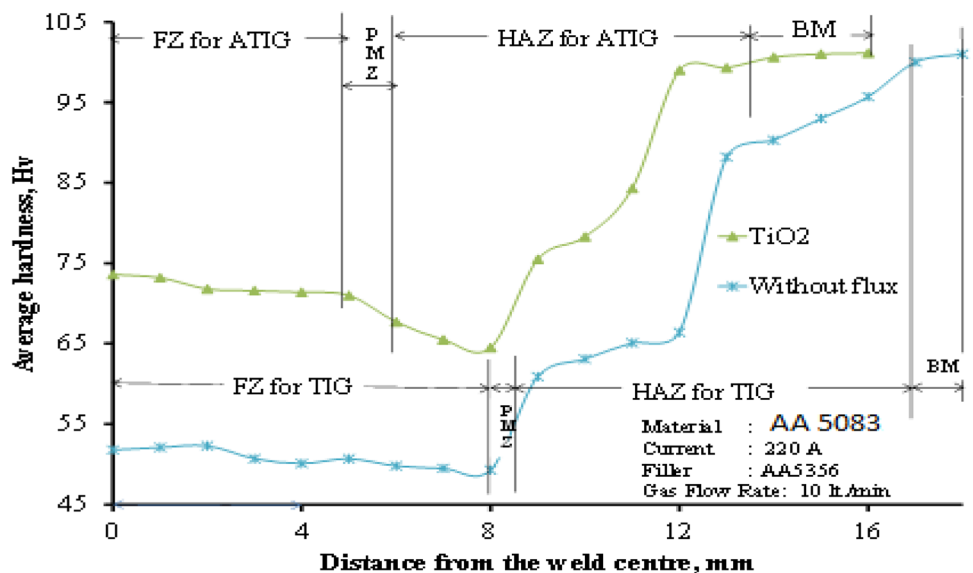


Fig. 9 SEM with EDS map of samples after welding **a** without flux **b** with TiO_2 flux

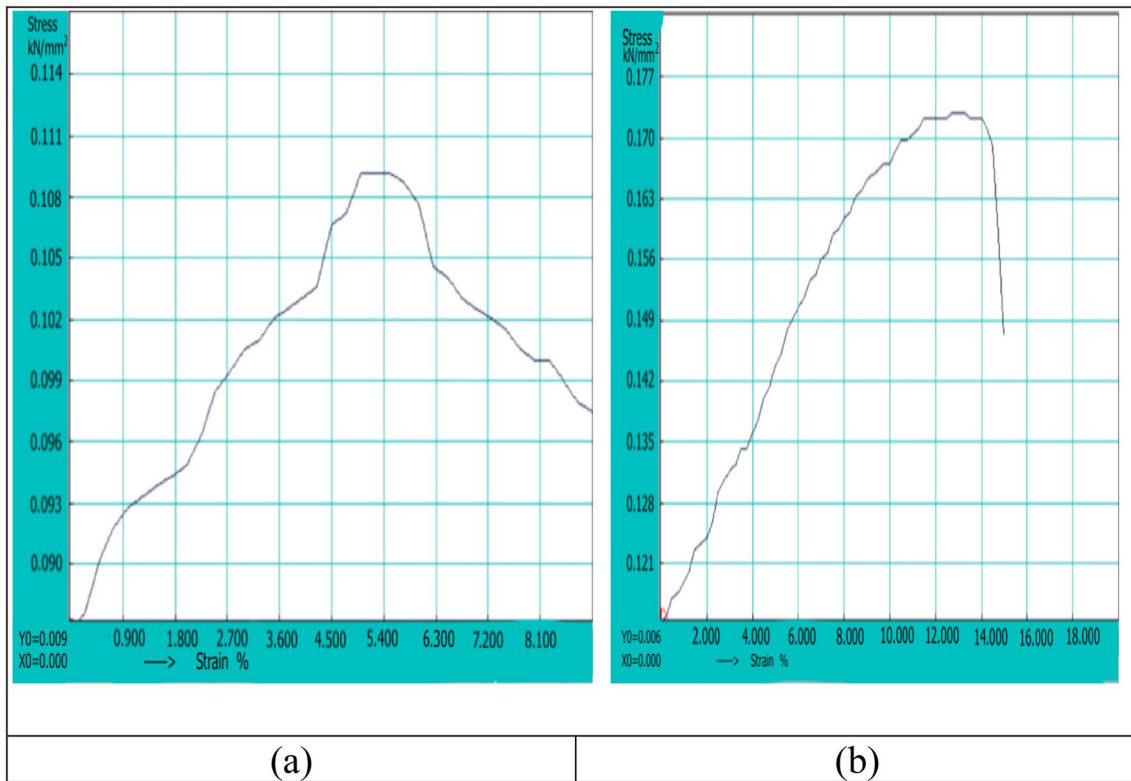
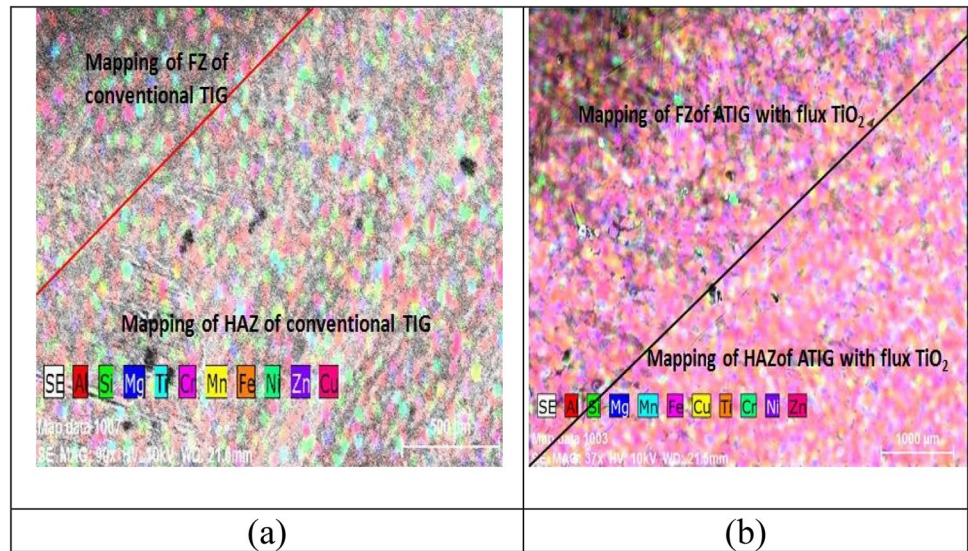


Fig. 10 Tensile graph of samples after welding **a** without flux **b** with TiO_2 flux

Scanning Electron Microscope—EDS

In this investigation, SEM–EDS mapping is utilized to characterize the BM and weldments as well as to determine the elemental composition of the BM, conventional TIG, and A-TIG with TiO_2 flux as shown in Fig. 9. Figure 9 displays the results of the SEM with EDS examination of BM AA 6061 and AA 5083.

In Fig. 9a the elements found are Zn, Si, Cu, Mg, Ni, Ti, Cr, and Fe. Mg and Si have been established as the principal elements of AA 6061. Mg, Zn, Si, and Cu have been confirmed as the principal elements in AA 5083. The specific alloying elements present in AA 5083, including magnesium, zinc, silicon, and copper, are carefully chosen to tailor the alloy’s properties to meet the requirements of diverse industrial applications. These elements work

in synergy to provide the alloy with its desired strength, corrosion resistance, and other essential characteristics. Understanding their significance helps in optimizing the performance of AA 5083 in various engineering and manufacturing contexts [24–26]. The lack of strengthening phases of Mg, Si, and Zn in FZ of conventional TIG and A-TIG welded samples presence of flux (TiO_2) is due to the dissolution. Figure 9a shows the composition of FZ and HAZ of conventional TIG. It is noted that grains are coarse in FZ, and alloy elements like Zn and Mg are greatly lost. It also observed that none of the A-TIG welded samples presence of flux (TiO_2) and BM had a significantly different composition of the FZ, as illustrated in Fig. 9b. The typical inter-granular precipitates of Fe, Mg, and Si are shown in Fig. 9b. The study of the EDS map shows that the Si, Ti, and Mg content of the nuclei is high Fig. 9b. Also Si is a component of the AA 6061 basic material. Excessive Ti is present in the matrix because TiO_2 powder is used as an activated flux [27, 28]. The Ti present in the matrix increases the hardness of the weld interface. A major portion of the weld interface is covered with aluminium. Coarse phases were recorded, richer in Si, Zn, Mg, Cu, and Cr in HAZ. After welding, the concentration of Mn, Zn, and Cu again decreases. But the use of filler rod AA 5356 and flux TiO_2 resulted in a modest rise in the concentration of Ti and Si [29, 30]. The utilization of SEM–EDS mapping in this investigation enhances our understanding of the intricate interactions between welding processes, materials, and resulting microstructures. It provides valuable data to support our findings on the effects of welding parameters, such as flux usage, on the composition and structure of weldments.

Effect of Tensile Strength

The tensile strength of the standard ATIG with fluxes (TiO_2) and TIG is confirmed in Fig. 10a, b to be 114 and 177 MPa, respectively. Additionally, it is noted that the ATIG welded junction has a higher ultimate tensile strength than traditional TIG. When compared to other ATIG welded samples, the AA 6061 and AA 5083 samples with flux TiO_2 have the highest tensile strength. It agrees well with [31]. Conventional TIG joints' average stressing was 4% lower than ATIG joints' with (SiO_2 & TiO_2) 18% and 7%, respectively.

Conclusion

The AA 6061-AA 5083 dissimilar welding was successfully finished utilizing the A-TIG technique. According to the experiment, the following conclusion was drawn:

1. The dissimilar joint between AA 6061 and AA 5083 was produced without any significant welding flaws. When compared to traditional TIG welding, ATIG welding revealed higher DOP.
2. The experimental results indicate that the weld junction created through the use of A TIG with flux TiO_2 on AA 6061 and AA 5083 materials exhibits a significantly higher ultimate tensile strength of 177 MPa, surpassing the traditional TIG welding technique without flux, which yielded a tensile strength of 114 MPa. This suggests that the incorporation of flux in A TIG welding process enhances the mechanical integrity of the welded joint, resulting in a superior ultimate tensile strength when compared to conventional TIG welding.
3. The negative impact of AA 5356 filler on getting superior mechanical characteristics is very significant due to Mg's role as a significant alloying element.
4. The TiO_2 activated flux enhanced the hardness of the weld interface above base metal, according to the microstructure study using EDS and SEM.
5. Overdue to the dissimilar alloys' reduced ability to dissolve, the dissimilar weld proves that oxides generated during welding as a result of the AA 6061-AA 5083 dissimilarity.

Funding There is no funding received from any source to conduct this research work.

Declarations

Conflict of interest There is no conflict of interest in this research work.

References

1. P. Vasantharaja, M. Vasudevan, Studies on A-TIG welding of low activation ferritic/martensitic (LAFM) steel. *J. Nucl. Mater.* **421**(1), 117–123 (2012)
2. G. Chandrasekar, C. Kailasanathan, D.K. Verma, Investigation on un-peened and laser shock peened weldment of Inconel 600 fabricated by ATIG welding process. *Mater. Sci. Eng., A* **690**, 405–417 (2017)
3. H. Fazlinejad, A. Halvae “Effect of Zinc Oxide on Characteristics of Active Flux TIG Welds of 1050 Aluminum Plates” *World Academy of Science, Engineering and Technology International Journal of Materials and Metallurgical Engineering Vol:13, No:2*, 2019
4. Sudhanshu Ranjan Singh, Pradeep Khanna A-TIG (activated flux tungsten inert gas) welding: – A review *Materials Today Volume 44, Part 1*, 2021,
5. Balram Yelamasetti, G. Rajyalakshmi “Effect of TIG, pulsed TIG and Interpulse TIG welding techniques on weld strength of dissimilar joints between Monel 400 and AISI 316” August 2019

- Materials Today Proceedings DOI:<https://doi.org/10.1016/j.matpr.2019.08.125>
6. Bijoy Rajak, Kaushal Kishore, Vipin Mishra "Investigation of a novel TIG-spot welding vis-à-vis resistance spot welding of dual-phase 590 (DP 590) steel: Processing-microstructure-mechanical properties correlation Materials Chemistry and Physics Volume 296, 15 February 2023, 127254
 7. Huang, H.Y., 2010. Effects of activating flux on the welded joint characteristics in gas metal arc welding. *Materials & Design* (1980–2015), 31(5), pp.2488–2495.
 8. Bhavin Shah BhaveshMadhvani "A Review Paper on A-TIG Welding Process" *IJSTE - International Journal of Science Technology & Engineering | Volume 3 | Issue 09 | March 2017* ISSN (online): 2349–784X.
 9. K.D. Ramkumar, B.M. Kumar, M.G. Krishnan, S. Dev, A.J. Bhalodi, N. Arivazhagan, S. Narayanan, Studies on the weldability, microstructure and mechanical properties of activated flux TIG weldments of Inconel 718. *Mater. Sci. Eng., A* **639**, 234–244 (2015)
 10. Sathavornvichit, N., Bookkamana, P. and Plubin, B., 2006, June. Central composite design in optimization of the factors of automatic flux cored arc welding for steel ST37. In *Proceedings of the 2nd IMT-GT regional conference on mathematics, statistics and applications*, Universiti Sains Malaysia, Penang (pp. 1–7).
 11. A. Kumar, S. Sundarajan, Selection of welding process parameters for the optimum butt-joint strength of an aluminum alloy. *Mater. Manuf. Processes* **21**(8), 779–782 (2006)
 12. Velaphi msomi, Nontle Mbana "Mechanical Properties of Friction Stir Welded AA1050-H14 and AA5083-H111 Joint: Sampling Aspect" Special Issue "Advanced Welding Technology in Metals" *Metals* 2020, 10(2), 214; <https://doi.org/10.3390/met1020214>
 13. Bansal A., Vettivel, S.C., Kumar, M., & Agarwal, M. (2023)
 14. Weld defect identification and characterization in radiographic images using deep learning *Engineering Research Express*
 15. W. Lucas, *TIG and plasma welding process—process technique, recommended practices, and applications*, 1st edn. (Woodhead Publishing, Cambridge, 1990)
 16. Yulong, L., Hua, Z., RongHua, H. and Jianning, X., 2008, December. Development of a steel rapid prototyping system based on TIG welding deposition technology. In *Knowledge Acquisition and Modeling Workshop, 2008. KAM Workshop 2008. IEEE International Symposium on* (pp. 154–157). IEEE.
 17. Yuvaraj, N., and Aravindan. S., "Comparison studies on mechanical and wear behavior of fabricated aluminum surface nano composites by fusion and solid state processing" *Surface and Coatings Technology*, 2017, pp. 309–319.
 18. D. Maissonnette, D. Bardel, V. Robin, D. Nelias, M. Suery, Mechanical behaviour at high temperature as induced during welding of a 6xxx series aluminium alloy. *Int. J. Press. Vessels Pip.* **149**, 55–65 (2017)
 19. Yiming, Huang., Wu, Di., Zhang, Zhifen., Chen, Huabin., and Chen, Shanben., "EMD-based pulsed TIG welding process porosity defect detection and defect diagnosis using GA-SVM." *Journal of Materials Processing Technology*, Vol.239, 2017, pp. 92–102.
 20. Chen, J., Zong, R., Wu, C., Padhy, G.K., and Hu, Q., 2016. Influence of low current auxiliary TIG arc on high speed TIG-MIG hybrid welding. *Journal of Materials Processing Technology*.
 21. Huang, Y., Wu, D., Lv, N., Chen, H. and Chen, S., 2016. Investigation of porosity in pulsed GTAW of aluminum alloys based on spectral and X-ray image analyses. *Journal of Materials Processing Technology*.
 22. T. Luijendijk, Welding of dissimilar aluminium alloys. *J. Mater. Process. Technol.* **103**, 29–35 (2000)
 23. A. Bansal, B.S. Pabla, S.C. Vettivel, Effect of TIG welding process parameters on Tensile behaviour of 5XXX and 6XXX series Aluminium Alloys : A Review. *Research Journal of Engineering and Technology* **9**(1), 1–8 (2018)
 24. R.R. Ambriz, D. Chicot, N. Benseddiq, G. Mesmacque, S.D. De la Torre, Local mechanical properties of the 6061–T6 aluminium weld using micro-traction and instrumented indentation. *European Journal of Mechanics-A/Solids* **30**(3), 307–315 (2011)
 25. Gómora, C.M., Ambriz, R.R., Curiel, F.F. and Jaramillo, D., 2017. Heat distribution in welds of a 6061-T6 aluminum alloy obtained by modified indirect electric arc. *Journal of Materials Processing Technology*.
 26. H. Fujii, T. Sato, S. Lu, K. Nogi, Development of an advanced A-TIG (AA-TIG) welding method by control of Marangoni convection. *Mater. Sci. Eng., A* **495**(1), 296–303 (2008)
 27. Kyama Praneetha, Maddela Apoorva, Thumpuru Prasan na Laxmi, S. Ravi Sekhar, S. Sravan Sashank "Experimental investigation on aluminium alloy AA6082 and AA2014 using the friction stir welding" *Mechanical Engineering*, Gokaraju Rangaraju Institute of Engineering and Technology, Hyderabad, India Available online 26 April 2022, Version of Record 23 June 2022.
 28. M. Srivastava, N. Khan, S. Nabi, S. Rathee, Microstructure and mechanical properties of friction stir welded Al–Mg–Si alloys under variable parameter conditions. *J. Inst. Eng. India Ser. D* 1–12, (2023).
 29. S.W. Shyu, H.Y. Huang, K.H. Tseng, C.P. Chou, Study of the performance of stainless steel A-TIG welds. *J. Mater. Eng. Perform.* **17**(2), 193–201 (2008)
 30. P. Pankaj, A. Tiwari, L.N. Dhara, S. Raj, P. Biswas, Investigations on the effect of sheets positioning in advancing & retreating side for dissimilar FSW of DH36 steel and aluminum alloy 6061. *J. Inst. Eng. India Ser. C* **103**(1), 5–20 (2022)
 31. Kumar, R., Vettivel, S.C., & Kumar Kansal, H. (2021) Effect of SiO₂ flux on the depth of penetration, microstructure, texture and mechanical behaviour of AA 6063 T6 aluminium alloy using activated TIG welding. *Bulletin of the polish Academy of Sciences Technical Sciences*, e 136215-e136215

Publisher's Note Springer Nature remains neutral with regard to jurisdictional claims in published maps and institutional affiliations.

Springer Nature or its licensor (e.g. a society or other partner) holds exclusive rights to this article under a publishing agreement with the author(s) or other rightsholder(s); author self-archiving of the accepted manuscript version of this article is solely governed by the terms of such publishing agreement and applicable law.